J. Electrochem. Sci. Eng. ***00(0)*** *(2025) 2621; https://doi.org/10.5599/jese.2621*

Open Access : : ISSN 1847-9286

www.jESE-online.org

Original scientific paper

Electrochemical performance evaluation of $ZnCo_2O_4$ nanoflakes for hybrid supercapacitors

Deependra Jhankal[1,2], Bhanu Yadav[1], Preeti Shakya[3], Mohammad Saquib Khan[4], Krishna Kumar Jhankal[5] and Kanupriya Sachdev[1,3,✉]

[1]*Department of Physics, Malaviya National Institute of Technology, Jaipur 302017, India*
[2]*Department of Physics, School of Applied Science, Suresh Gyan Vihar University, Jaipur, 302017 India*
[3]*Materials Research Centre, Malaviya National Institute of Technology, Jaipur 302017, India*
[4]*Department of Sustainable Energy Engineering, Indian Institute of Technology, Kanpur 208016 India*
[5]*Department of Chemistry, University of Rajasthan, Jaipur 302004, India*

Corresponding Author: ✉ *ksachdev.phy@mnit.ac.in*

Received: December 31, 2024; Revised: December 24, 2025; Published: December 28, 2025

Abstract

This study focuses on the synthesis and characterization of zinc cobaltite ($ZnCo_2O_4$) as an electrode material for supercapacitor (SC) applications. $ZnCo_2O_4$ was synthesized via an efficient sol-gel method, followed by annealing. Morphological and structural characterrizations revealed that $ZnCo_2O_4$ forms as nanoflakes with a well-crystallized structure. Electrochemical parameters of $ZnCo_2O_4$ were examined by various electrochemical techniques in a 3 M KOH aqueous electrolyte. The highest specific capacitance (C_{sp}) of 321 F g^{-1} was obtained at a current density of 0.8 A g^{-1}. The electrochemical performance of the $ZnCo_2O_4$ electrode is superior, owing to its porous nanoflake morphology, which provides numerous active sites and enables substantial charge storage. Moreover, multiple oxidation states of Zn and Co enhance redox reactions at the electrode surface, thereby improving the electrode's pseudocapacitance. The superior electrochemical performance of $ZnCo_2O_4$ indicates that it is a promising cathode material for hybrid SC devices.

Keywords

Bimetal oxide; energy storage; specific capacitance; cyclic stability; energy density; power density

Introduction

Along with significant technological advancements and population growth, global energy consumption is rising rapidly. Compared with fossil fuels, environmentally friendly energy sources such as solar,

biomass, hydro, and wind power are a smart choice for energy supply; however, these sources are intermittent, making energy storage devices essential for achieving a sustainable energy system [1].

Among various energy storage systems, supercapacitors (SCs) deliver better frequency response, indefinite charge/discharge cycles, and excellent dielectric strength. SCs have 10-100 times higher energy storage capacity than capacitors. Compared with lithium-ion batteries, SCs offer higher peak currents, lower cost per cycle, better reversibility, a corrosion-resistant electrolyte, minimal material toxicity, and no damage from overcharging [2-4]. While batteries are less expensive to acquire and maintain a steady voltage during discharge, they also require sophisticated electronic management and switching systems, which result in energy loss and spark risk. Hence, SCs, with their superior power density and cyclic stability, have attracted considerable interest, offering a significant opportunity to develop higher-performing hybrid SCs (HSCs) [5-7].

HSCs exhibit greater power and energy density than capacitors and rechargeable power sources. Critical elements of HSC include electrode materials along with the morphology and specific surface area, the electrolyte, operating conditions and cell configuration. These factors affect charge-transfer kinetics and ion diffusion, thereby influencing cycle life, capacitance-voltage characteristics, specific surface area, and conductivity [8-10]. Additionally, HSCs exhibit specific challenges in cycle performance, and it can be challenging to identify appropriate positive and negative electrode materials [11].

Bimetal oxides (BMOs) are a class of oxide materials that consist of two different metallic elements and have the general formula AB_2X_4, with a spinel structure. In recent years, BMOs have received attention, as their chemical composition offers greater flexibility to attain novel electrical, chemical and magnetic properties as compared to other metal oxides. BMOs can be synthesized with a variety of compositions and structures, enabling tailoring of their properties to specific applications [12]. Recently, BMOs have been studied as potential electrode materials for lithium-ion batteries and SCs because they offer high capacity and excellent cycling stability for energy storage applications. Moreover, BMOs have also been investigated for their ability to connect solar energy to drive chemical reactions [9].

Among suitable materials for SC electrodes, Co_3O_4 is a promising material due to its very high theoretical specific capacitance (C_{sp}) of 3650 F g^{-1}. However, it has several disadvantages, including lower electrical conductivity, a short cycle life, and a low electrode material density [13]. BMOs with spinel structures are produced by partially replacing Co in Co_3O_4 with transition elements such as Mn, Ni, Zn, Fe, *etc*. Among various spinel BMOs, zinc cobaltite ($ZnCo_2O_4$) has been widely utilized for HSC applications because of its outstanding redox activity, good conductivity, and large theoretical C_{sp} of 2650 F g^{-1}. Additional advantages include the potential for synthesis from inexpensive precursors and readily available materials. Spinel cobaltite $ZnCo_2O_4$ is known to be efficient for oxygen reduction when used as an electrode, and is low-cost, abundant, and environmentally friendly. $ZnCo_2O_4$ has been developed for applications in Li-ion batteries, electrocatalysis, and SCs, thereby demonstrating its multifunctionality. It was revealed that both $NiCo_2O_4$ and $ZnCo_2O_4$ electrodes exhibited superior capacitive performance compared with Co_3O_4, owing to their greater electrochemical activity and richer redox reactions [14-16].

Here, the sol-gel synthesis strategy was adopted to synthesize the spinel $ZnCo_2O_4$. Electrochemical parameters of $ZnCo_2O_4$ were investigated in KOH solution as a single electrode and in a symmetric ($ZnCo_2O_4$ || $ZnCo_2O_4$) device using cyclic voltammetry (CV) and galvanostatic charge-discharge (GCD) techniques.

Experimental

Reagents

Sodium hydroxide (NaOH), cobalt nitrate hexahydrate ($Co(NO_3)_2{\cdot}6H_2O$), Zn nitrate trihydrate ($Zn(NO_3)_2{\cdot}3H_2O$), carboxymethyl cellulose sodium salt (CMC, high purity), potassium hydroxide (KOH), potassium hexacyanoferrate(III) ($K_3Fe(CN)_6$) and glycerol were acquired from Alfa Aesar (Thermo Scientific Chemicals, U.S.). Britton-Robinson (BR) buffer solution (pH ~7) was prepared by mixing equal volumes of 0.04 M boric acid (0.248 g in 100 ml), 0.04 M phosphoric acid (0.26 ml in 100 ml), and 0.04 M acetic acid (0.23 ml in 100 ml) in a 500 ml volumetric flask, that is titrated to the desired pH with 0.2 M sodium hydroxide.

Synthesis of $ZnCo_2O_4$

$ZnCo_2O_4$ was synthesized by an efficient sol-gel strategy. A 0.20 M NaOH solution was prepared in 200 ml of deionised water (DI). Simultaneously, 0.10 M $Co(NO_3)_2{\cdot}6H_2O$ and 0.05M ($Zn(NO_3)_2{\cdot}3H_2O$) were prepared in 100 ml DI water and dropped into NaOH solution under continuous stirring. After 30 minutes, 10 ml of glycerol was introduced to prevent particle agglomeration. The resulting mixture was stirred at 80 °C for 90 minutes. The collected material was washed with DI water and dried at 80 °C. Subsequently, the material was finely powdered through grinding. Finally, the prepared material was annealed at 450 °C for 3 hours to yield a black $ZnCo_2O_4$ powder. Figure 1 shows the schematic of the step-by-step preparation of $ZnCo_2O_4$.

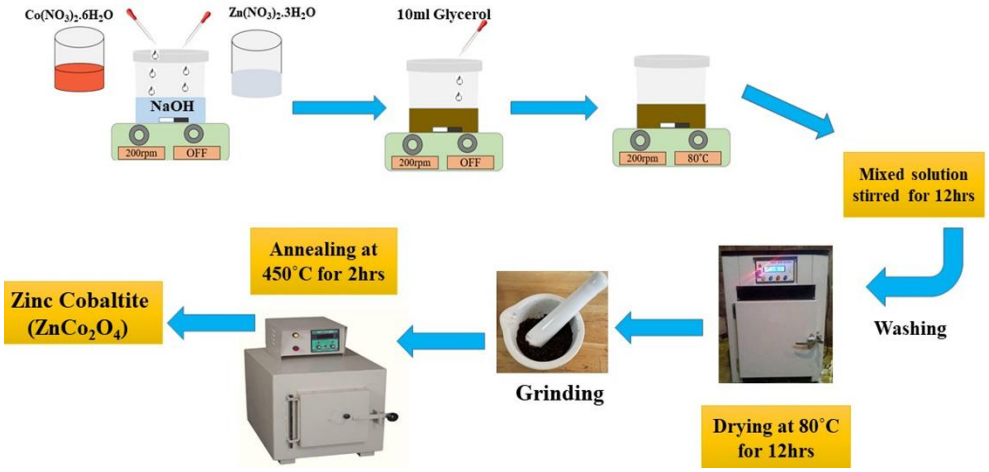

***Figure 1**. Schematic diagram of sol-gel method for preparation of $ZnCo_2O_4$*

Characterization techniques

X-ray diffraction (XRD) was used by utilizing a Panalytical X-Pert Pro diffractometer (Malvern Panalytical, Netherlands) to examine the crystallographic properties of the prepared sample. The microstructure analysis was evaluated by a field emission scanning electron microscope (FESEM), using a Nova Nano FESEM-450 (FEI Company, United States). The sample is also analysed by Raman spectroscopy (STR 500 Confocal Micro Spectrometer, λ = 532 nm) (TechnoS Photonics, India). Electrochemical characterizations, including CV and GCD, were performed using a Metrohm AUTOLAB PGSTAT30 workstation (Metrohm AG, Switzerland).

Fabrication of the electrode

Firstly, a slurry of $ZnCo_2O_4$ was prepared by mixing $ZnCo_2O_4$, CMC and acetylene black (Alfa Aesar, ≥ 99 %) with a ratio of 80:10:10 in 5 ml of isopropyl alcohol solution. The slurry was then coated onto Ni-foam (1×1 cm) and heated at 120 °C for 12 hours in an air oven (1 mg of active material *per*

cm² of Ni-foam). For the measurement of the active surface area of $ZnCo_2O_4$, $ZnCo_2O_4$/GCE was prepared by drop casting the slurry of $ZnCo_2O_4$ on a glassy carbon electrode (GCE) (diameter of 5 mm) (active mass of material is 0.4 mg) and drying at 60 °C for 1 hour. An electrochemical study of the $ZnCo_2O_4$ electrode was performed in a 3-electrode setup with an Ag/AgCl (3 M KCl) electrode as the reference and a Pt wire as the counter electrode, with 3 M KOH as the electrolyte. For measurement of temperature stability, a symmetric SC device ($ZnCo_2O_4||ZnCo_2O_4$) was constructed. The $ZnCo_2O_4$ slurry was drop-cast onto a stainless steel foil (2×2 cm) with an active material mass of 1 mg and dried at 80 °C for 6 hours to prepare electrodes. The two similar electrodes were sandwiched with KOH-soaked Whatman filter paper in the middle of the electrodes, and finally, the device was sealed with parafilm.

Results and discussion

The effective surface area of $ZnCo_2O_4$ modified glassy carbon electrode

The cyclic voltammograms of 0.1 mM $K_3[Fe(CN)_6]$ in BR buffer (pH 7) were recorded at $ZnCo_2O_4$/GCE and bare GCE to determine their effective surface areas (Figure 2). The Randles-Ševčik Equation (1) provides a relationship between peak current, scan rate, and surface area of the electrode [17]:

$$I_p = (2.69\times10^5)n^{3/2}AD_o^{1/2}\nu^{1/2}C \quad (1)$$

where I_p / A refers to the maximum peak current, n is the number of electrons transferred in the electrode reaction, A / cm^2 shows the effective surface area of the working electrode, D_o / cm^2 s^{-1} is the diffusion coefficient in (D_o for $K_3[Fe(CN)_6]$ = 7.6×10^{-6} cm^2 s^{-1}), ν / V s^{-1}indicates the scan rate, while C / mol cm^{-3}represents the concentration of $K_3[Fe(CN)_6]$. The evaluated surface area of $ZnCo_2O_4$/GCE was 0.0767 cm^2. This value is approximately 3 times higher than that of a bare GCE (0.0266 cm^2), due to the flakes-like micro-structure of $ZnCo_2O_4$ [18].

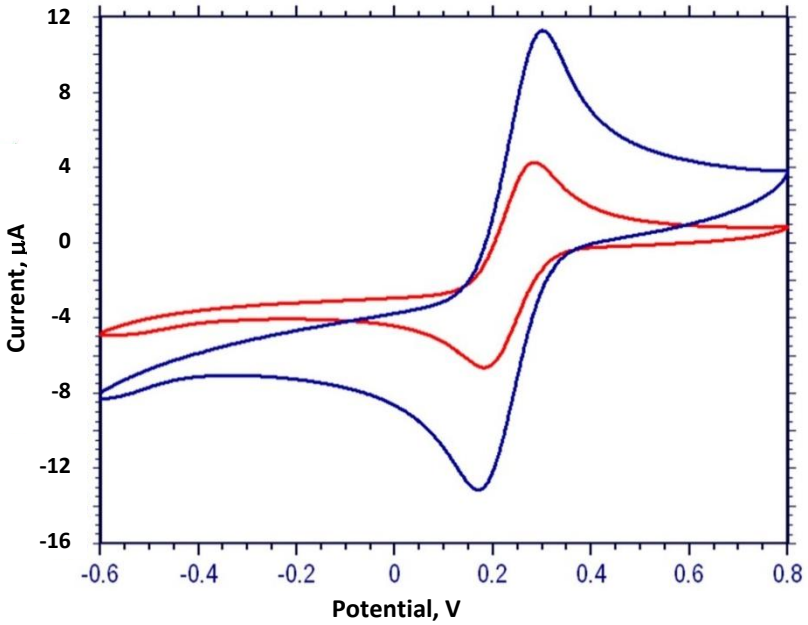

Figure 2. *Cyclic voltammograms of 0.1 mM $K_3[Fe(CN)_6]$ in BR buffer, pH 7 solution at $ZnCo_2O_4$/GCE (in blue) and bare GCE (in red)*

Figures 3a and b depict the FE-SEM results of $ZnCo_2O_4$, indicating the flake morphology of $ZnCo_2O_4$. The flake morphology of $ZnCo_2O_4$ enhances electrode performance by facilitating a large contact area

at the electrode-electrolyte interface. The XRD spectrum of $ZnCo_2O_4$ (Figure 2c) shows diffraction peaks at 19.07, 31.47, 36.96, 45.06, 55.66, 59.59, 65.18, and 77.54° corresponding to (111), (220), (311), (400), (422), (511), (440), and (533) planes, respectively. The positions and intensities of the peaks are well correlated with the cubic spinel structure of ZnCo2O4, as indexed by the JCPDS card number 01-1149 [19]. In the Raman spectra of $ZnCo_2O_4$ (Figure 2d), two intense peaks are observed relating to F_{2g} (518 cm^{-1}) and A_{1g} (684 cm^{-1}), corresponding to symmetrical modes of $ZnCo_2O_4$.

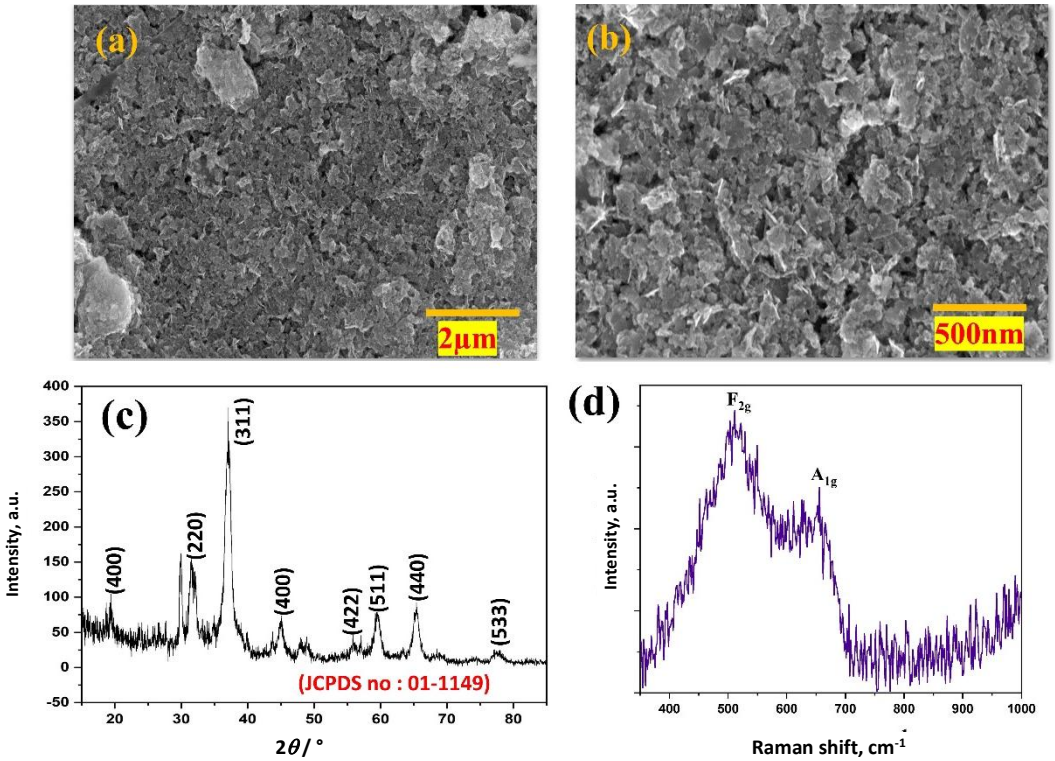

Figure 3. *(a) and (b) FE-SEM images at different resolutions, (c) XRD pattern and (d) Raman spectrum of spinel $ZnCo_2O_4$*

Figure 4a illustrates CV profiles of the $ZnCo_2O_4$ electrode in 3M KOH at different sweep rates (5 to 300 mV s^{-1}). CV curves exhibit redox peaks with a quasi-rectangular shape, indicating that charge-storage kinetics are largely diffusion-controlled. Moreover, the CV profiles maintain their characteristic shapes, indicating good reversibility of the electrode material [20]. Equations (1) to (3) serve as the foundation for the possible electrochemical redox reaction in an alkaline solution [21].

$$ZnCo_2O_4 + H_2O + OH^- \leftrightarrow 2CoOOH + ZnOOH + e^- \quad (1)$$

$$ZnOOH + OH\text{-} \leftrightarrow ZnO_2 + H_2O + e^- \quad (2)$$

$$CoOOH + OH^- \leftrightarrow CoO_2 + H_2O + e^- \quad (3)$$

The nonlinear shapes of GCD curves (Figure 3b) illustrate the pseudocapacitive/diffusive behaviour of the ZnCo2O4 electrode, indicating battery-type performance of the material.

The specific capacitance (C_{sp}/F g^{-1}) of the $ZnCo_2O_4$ electrode in a three-electrode cell was extracted by utilizing Equation (4):

$$C_{sp} = \frac{i\Delta t}{m\Delta V} \quad (4)$$

Here Δt / s and ΔV / V exemplify discharge time and cell voltage, respectively, while the (i/m) / A g^{-1} is gravimetric current density (CD). The calculated C_{sp} values for different applied CDs are shown in Figure 4(c). The $ZnCo_2O_4$ electrode possesses a maximum C_{sp} of 321.4 F g^{-1} at a CD of 0.8 A g^{-1}. The value of C_{sp} decreases at higher CD and attains a minimum C_{sp} of 100 F g^{-1} at a CD of 8 A g^{-1}. The high value of C_{sp}, along with the significant energy density of the $ZnCo_2O_4$ electrode, is attributable to the

multiple valence states of Zn and Co, which enhance faradaic reactions, resulting in superior capacitive performance of the material.

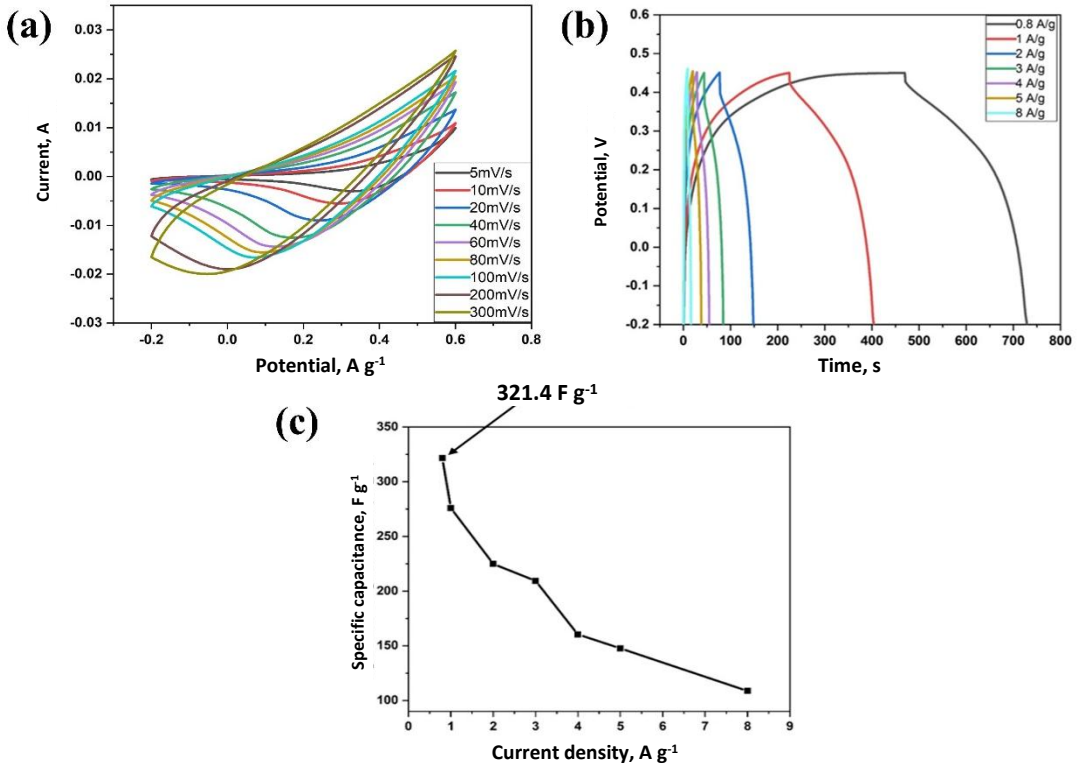

Figure 4. *(a) CV profiles of $ZnCo_2O_4$ electrode in BR solution at different scan rates, (b) GCD curves at different applied current densities, (c) specific capacitance values in dependence on applied current density*

Equation (5) (Dunn's method) was applied to determine the separate contributions of current responses at a fixed voltage that result from the capacitive-controlled and diffusion-controlled charge storage mechanisms.

$$i_p = a_1 \nu + a_2 \nu^{1/2} \quad (5)$$

Here, $a_1\nu$ and $a_2\nu^{1/2}$ represent current contributions from diffusive and capacitive kinetic processes, respectively [20,21]. The constants a_1 and a_2 were evaluated by the linear fit of i_p/ν *vs.* $\nu^{1/2}$ curve. Where the slope of the curve gives the value of constant a_1 and the intercept of the curve gives the value of constant a_2. Figure 5(a) shows this linear plot for the $ZnCo_2O_4$ electrode at 0.1 V. The capacitive and diffusion current contributions at various scan rates are demonstrated in Figure 5(b).

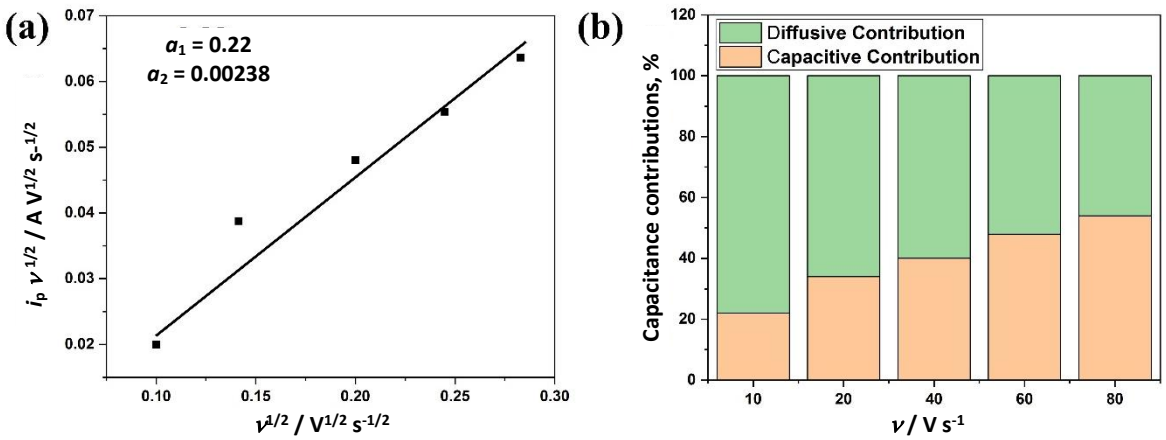

Figure 5. *(a) Linear fit of $i/\nu^{1/2}$ vs. $\nu^{1/2}$ for $ZnCo_2O_4$ electrode at 0.1 V;(b) contributions of capacitance due to capacitive and diffusive processes at different scan rates*

The dominance of the diffusive contribution to the total current response at lower scan rates indicates that the nature of charge storage is largely diffusive-controlled (battery type).

Figure 6(a) represents the results of electrode cyclization, *i.e.* the effects of 50 to 1500 CV cycles performed at a scan rate of 100 mV s^{-1} to the $ZnCo_2O_4$ electrode in 3M KOH. The percentage of capacitance retention of the $ZnCo_2O_4$ electrode over 1500 cycles is depicted in Figure 7(b), which indicates the $ZnCo_2O_4$ electrode retains approximately 92 % efficiency after 1500 CV cycles. The $ZnCo_2O_4$ electrode exhibits better cycle retention owing to its unique morphology and multiple redox sites.

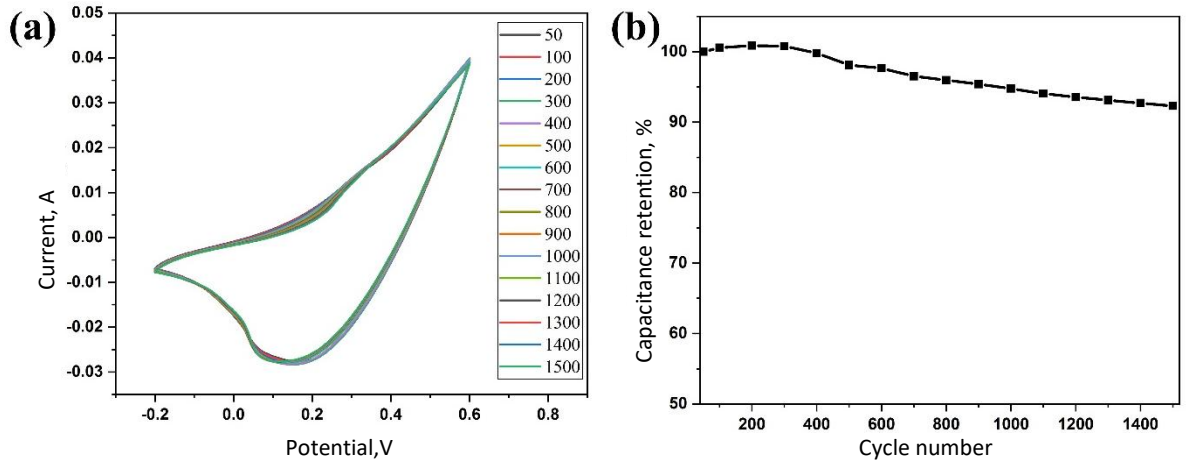

Figure 6. *(a) CVs of 50 to 1500 cycles preformed at 100 mV s^{-1} to $ZnCo_2O_4$ electrode in 3M KOH and (b) retention of cyclic stability over 1500 CV cycles*

To evaluate the temperature adaptability of $ZnCo_2O_4$, a symmetric supercapacitor device ($ZnCo_2O_4||ZnCo_2O_4$) was constructed and a GCD curve was recorded at different temperatures (10, 20 and 30 °C) at the current density of 0.2 A g^{-1}. The GCD profiles of the fabricated symmetric SC device are presented in Figure 7a. The specific capacitance values of a single electrode of a two-electrode (symmetric) cell (C_{sp}), were calculated by Equation (6) and depicted in Figure 7b.

$$C_{sp} = \frac{4i\Delta t}{m\Delta V} \tag{6}$$

In Equation (6), m is the mass of both electrodes. It can be noted that variations of C_{sp} values with temperature change are relatively small, and the maximum C_{sp} of 77.6 F g^{-1} at 0.2 A g^{-1} is attained at 20 °C.

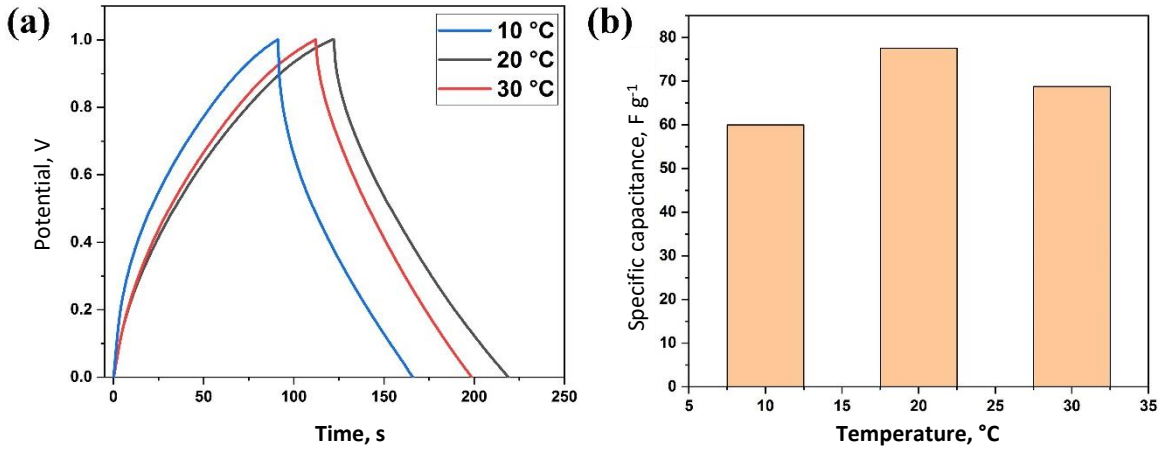

Figure 7. *(a) GCD curves at 0.2 A g^{-1} of fabricated device ($ZnCo_2O_4||ZnCo_2O_4$) and (b) C_{sp} values at different temperatures*

A comparative study presented in Table 1 shows that the electrochemical performance of $ZnCo_2O_4$ as a cathode material is comparable to, or better than, that reported in the published literature. The nanoflake morphology, providing a large number of diffusion channels for fast ion movement and the presence of multiple oxidation states of Zn and Co, is giving rise to fast Faradic redox reactions resulting in improved capacitance value of $ZnCo_2O_4$ electrode.

Table 1. *Comparison of specific capacitance values and morphology of $ZnCO_2O_4$ electrode obtained from the literature data and this work*

Method of synthesis	Morphology	Electrolyte	Capacitance, F g^{-1}	Measurement cell configuration	Ref.
Co-precipitation route	Nanostructure	2 M KOH	159 at 2 mA cm^{-2}	Three-electrode	[22]
Hydrothermal	Nanomaterial	2 M KOH	290.5 at 0.5 A g^{-1}	Three-electrode	[23]
Hydrothermal	Nanorods	3 M KOH	10.90 at 10 mV s^{-1}	Three-electrode	[24]
Co-precipitation method	Nanomaterial	6 M KOH	77 at 5 mV s^{-1}	Two-electrode	[25]
Solvothermal	Nanoparticles	6 M KOH	451 at 5 mV s^{-1}	Three-electrode	[26]
Effective and additive-free	Hierarchical peony-like	3 M KOH	440 at 1 A g^{-1}	Three-electrode	[27]
Solvothermal	Hollow microspheres		78.89 mAh g^{-1} at 1 A g^{-1}	Two-electrode	[28]
Hydrothermal	Microspheres	1 M KOH	593 at 10 mV s^{-1}	Three-electrode	[21]
Sol-gel method	Nanoflakes	3 M KOH	321.4 at 0.8 A g^{-1}	Three-electrode	This work

Conclusion

$ZnCo_2O_4$, as an electrode material for supercapacitor applications, was successfully synthesized via an effective sol-gel technique. The FE-SEM, XRD and Raman studies showed that the prepared $ZnCo_2O_4$ has flake morphology along with a spinel cubic crystal structure. The $ZnCo_2O_4$ electrode exhibited good electrochemical performance with a C_{sp} of 321.4 F g^{-1} at a current density of 0.8 A g^{-1}. Moreover, the $ZnCo_2O_4$ electrode possesses capacitance retention of 92 % over 1500 CV cycles. The extraordinary characteristics of the $ZnCo_2O_4$ electrode come from the porous microstructure of $ZnCo_2O_4$, which not only enhances the contact area of the electrode-electrolyte interface but also facilitates the numerous active channels for faradic redox reactions. Multiple valencies of Zn and Co are an additional advantage. These results fully confirm the possibility of $ZnCo_2O_4$ as a significant electrode material for hybrid SC devices. This work supports the development of a prospective routine for constructing next-generation advanced-energy storage systems. Additionally, this work provides a comprehensive overview of the synthesis of various metal oxides and sulphides for practical hybrid SC device applications.

Acknowledgements: *For providing the materials characterization facilities, the authors would like to thank the MRC (Materials Research Centre) at MNIT Jaipur.*

Funding: *Not applicable.*

Conflict of interest: *The authors express no conflict of interest.*

References

[1] M. Wayu, Manganese Oxide Carbon-Based Nanocomposite in Energy Storage Applications, *Solids* **2** (2021) 232-248. https://doi.org/10.3390/solids2020015

[2] S. Zhang, N. Pan, Supercapacitors performance evaluation, *Advanced Energy Materials* **5(6)** (2015) 1401401. https://doi.org/10.1002/aenm.201401401

[3] Y. Zhang, S. Hu, C. Li, X. Yan, Y. Zhang, R. Yin, Y. Wei, K. Gao, H. Gao, Advanced strategies for

enhancing electrochemical performance of NiAl LDH electrodes in supercapacitors, *Coordination Chemistry Revews* **531** (2025) 216497. https://doi.org/10.1016/j.ccr.2025.216497

[4] Y. Zhang, X. Jing, X. Yan, H. Gao, K. Gao, Y. Cao, S. Hu, Y. Zhang, Rational design of NiMn-based electrode materials for high-performance supercapacitors, *Coordination Chemistry Reviews* **499** (2024) 215494. https://doi.org/10.1016/j.ccr.2023.215494

[5] L. Zhang, X. Hu, Z. Wang, F. Sun, D. G. Dorrell, A review of supercapacitor modeling, estimation, and applications: A control/management perspective, *Renewable and Sustainable Energy Reviews* **81** (2018) 1868-1878. https://doi.org/10.1016/j.rser.2017.05.283

[6] Y. Zhang, Y. Zhang, C. Li, X. Yan, S. Hu, R. Yin, Y. Wei, K. Gao, H. Gao, Research progress of $NiFe_2O_4$ electrode materials in supercapacitors: Preparation, modification, structural regulation, and future challenges, *Coordination Chemistry Reviews* **519** (2024) 216103. https://doi.org/10.1016/j.ccr.2024.216103

[7] Y. Zhang, C. Zhou, X. Yan, Y. Cao, H. Gao, H. Luo, K. Gao, S. Jue, X. Jing, Recent advances and perspectives on graphene-based gels for superior flexible all-solid-state supercapacitors, *Journal of Power Sources* **565** (2023) 232916. https://doi.org/10.1016/j.jpowsour.2023.232916

[8] S. Ghosh, P. Samanta, P. Samanta, N. C. Murmu, T. Kuila, Investigation of Electrochemical Charge Storage Efficiency of $NiCo_2Se_4$/RGO Composites Derived at Varied Duration and Its Asymmetric Supercapacitor Device, *Energy and Fuels* **34** (2020) 13056-13066. https://doi.org/10.1021/acs.energyfuels.0c02152

[9] D. Jhankal, M. S. Khan, B. Yadav, P. Shakya, N. Bhardwaj, K.K. Jhankal, K. Sachdev, Diffusion kinetics of $CuCo_2O_4$ nanorods for next-generation solid state sodium-ion hybrid supercapacitor, *Energy Storage* **5** (2023) e482. https://doi.org/10.1002/est2.482

[10] S. Saha, P. Samanta, N. C. Murmu, T. Kuila, A review on the heterostructure nanomaterials for supercapacitor application, *Journal of Energy Storage* **17** (2018) 181-202. https://doi.org/10.1016/j.est.2018.03.006

[11] Y. Zhang, S. Xue, X. Yan, H. L. Gao, K. Gao, Preparation and electrochemical properties of cobalt aluminum layered double hydroxide/carbon-based integrated composite electrode materials for supercapacitors, *Electrochimica Acta* **442** (2023) 141822. https://doi.org/10.1016/j.electacta.2023.141822

[12] Y. Li, L. Xu, M. Jia, L. Cui, J. Gao, X.-J. Jin, Hydrothermal Synthesis and Characterization of Litchi-Like $NiCo_2Se_4$@carbon Microspheres for Asymmetric Supercapacitors with High Energy Density, *Journal of The Electrochemical Society* **165** (2018) 303-310. http://doi.org/10.1149/2.0991807jes

[13] X.-H. Xia, J.-P. Tu,Y.-Q. Zhang, Y.-J. Mai, X.-L. Wang, C.-D. Gu, X.-B. Zhao, Freestanding Co 3O 4 nanowire array for high performance supercapacitors, *RSC Advances* **2** (2012) 1835-1841. https://doi.org/10.1039/C1RA00771H

[14] S. Xiong, C. Yuan, X. Zhang, B. Xi, Y. Qian, Controllable synthesis of mesoporous Co_3O_4 nanostructures with tunable morphology for application in supercapacitors, *Chemistry-A European Journal* **15** (2009) 5320-5326. https://doi.org/10.1002/chem.200802671

[15] Y. A. Kumar, K. D. Kumar, H. J. Kim, Reagents-assisted ZnCo2O4 nanomaterial for supercapacitor application, *Electrochimica Acta* **330** (2020) 135261. https://doi.org/10.1016/j.electacta.2019.135261

[16] M. M. Faras, S. S. Patil, P. S. Patil, A. P. Torane, Unleashing the Potential of Binder-Free Hydrothermally Synthesized Marigold-Like $ZnCo_2O_4$ for Supercapacitors, *Journal of Energy Storage* **74** (2023) 109490. https://doi.org/10.1016/j.est.2023.109490

[17] R. Agarwal, D. Jhankal, R. K. Sharma, R. Yadav, D. K. Sharma, K. K. Jhankal, Voltammetric sensing probe using MoS2-rGO nanocomposite fabricated pencil graphite electrode for

electro-kinetic study of the antidepressant drug paroxetine in pharmaceuticals, *Ionics* **31** (2025) 2243-2258. https://doi.org/10.1007/s11581-024-05997-1

[18] R. Agarwal, D. Jhankal, R. Yadav, D. K. Sharma, K. K. Jhankal, Development of ZnO-adorned glassy carbon electrode for voltammetric sensing and electro-kinetic investigations of antihypertensive drug efonidipine, *Monatshefte für Chemie* **155** (2024) 17-28. https://doi.org/10.1007/s00706-023-03132-w

[19] J. Cheng, Y. Lu, K. Qiu, H.Yan, X. Hou, J. Xu, L. Han, X. Liu, J.-K.Kim, Y. Luo, Mesoporous $ZnCo_2O^4$ nanoflakes grown on nickel foam as electrodes for high-performance supercapacitors, *Physical Chemistry Chemical Physics* **17** (2015) 17016-17022. https://doi.org/10.1039/C5CP01629K

[20] D. Jhankal, M. Saquib, K. K. Jhankal, K. Sachdev, Charge storage kinetics of MoS_2 flower decorated reduced graphene oxide for quasi solid-state symmetric supercapacitor, *Journal of Physics and Chemistry of Solids* **173** (2023) 111117. https://doi.org/10.1016/j.jpcs.2022.111117

[21] N. Tiwari, S. Kadam, S. Kulkarni, Synthesis and characterization of $ZnCo_2O_4$ electrode for high-performance supercapacitor application, *Materials Letters* **298** (2021) 130039. https://doi.org/10.1016/j.matlet.2021.130039

[22] M. Silambarasan, P.S. Ramesh, D. Geetha, K. Ravikumar, H. E. Ali, H. Algarni, P. Soundhirarajan, K. V. Chandekar, M. Shkir, A Facile Preparation of Zinc Cobaltite ($ZnCo_2O_4$) Nanostructures for Promising Supercapacitor Applications, *Journal of Inorganic and Organometallic Polymers and Materials* **31** (2021) 3905-3920. https://doi.org/10.1007/s10904-021-02077-z

[23] A. J. C. Mary, A. C. Bose, Surfactant-assisted $ZnCo_2O_4$ nanomaterial for supercapacitor application, *Applied Surface Science* **449** (2018) 105-112. https://doi.org/10.1016/j.apsusc.2018.01.117

[24] H. Wu, Z. Lou, H. Yang, G. Shen, A flexible spiral-type supercapacitor based on $ZnCo_2O_4$ nanorod electrodes, *Nanoscale* **7** (2015) 1921-1926. https://doi.org/10.1039/C4NR06336H

[25] K. Karthikeyan, D. Kalpana, N. G. Renganathan, Synthesis and characterization of $ZnCo_2O_4$ nanomaterial for symmetric supercapacitor applications, *Ionics (Kiel)* **15** (2009) 107-110. https://doi.org/10.1007/s11581-008-0227-y

[26] S. Chen, M. Xue, Y. Li, Y. Pan, L. Zhu, D. Zhang, Q. Fang, S. Qiu, Porous $ZnCo_2O_4$ nanoparticles derived from a new mixed-metal organic framework for supercapacitors, *Inorganic Chemistry Frontiers* **2** (2015) 177-183. https://doi.org/10.1039/C4QI00167B

[27] Y. Shang, T. Xie, Y Gai, L. Su, L. Gong, H. Lv, F. Dong, Self-assembled hierarchical peony-like ZnCo2O4 for high-performance asymmetric supercapacitors, *Electrochimica Acta* **253** (2017) 281-290. https://doi.org/10.1016/j.electacta.2017.09.042

[28] Y. Shang, T. Xie, C. Ma, L. Su, Y. Gai, J. Liu, L. Gong, Synthesis of hollow $ZnCo_2O_4$ microspheres with enhanced electrochemical performance for asymmetric supercapacitor, *Electrochimica Acta* **286** (2018) 103-113. https://doi.org/10.1016/j.electacta.2018.08.025